SOVIET PHYSICS

USPEKHI

A Translation of Uspekhi Fizicheskikh Nauk

SOVIET PHYSICS USPEKHI VOL. 2 (68), NO. 4, pp. 505-635 JULY-AUGUST 1959

THE STRUCTURE OF NUCLEONS

D. I. BLOKHINTSEV, V. S. BARASHENKOV, and B. M. BARBASHOV

Usp. Fiz. Nauk **68**, 417-447 (July, 1959)

1. INTRODUCTION

IN 1935 Yukawa[1] advanced the hypothesis that nucleons interact by way of some intermediate meson field. The particles of this field, the mesons, have a mass μ that is smaller than the nucleon mass M by about an order of magnitude. From the point of view of this hypothesis an actual "physical nucleon" consists of a "bare" point nucleon surrounded by a meson field, just as a point electric charge is surrounded by an electric field. In corpuscular language one can say that around a nucleon there is a cloud of virtual mesons, just as around an electric charge there is a cloud of virtual photons and electron-positron pairs.

The probability of emission of a virtual meson decreases markedly when its momentum is larger than μc.* Therefore the uncertainty in the energy of the meson cloud is about $\Delta E \sim \mu c^2$, and the uncertainty in the momentum is $\Delta p \sim \mu c$. From this it follows that the lifetime of a virtual meson is $\Delta t \sim \hbar/\mu c^2$, and the width of the meson field is $\Delta x \sim \hbar/\mu c$.

The discovery of charged and neutral π mesons (pions) with mass $m_\pi = M/6.3$ confirmed Yukawa's fundamental hypothesis, and the mathematical formulation of Yukawa's idea proposed in recent years by Chew and Low for nonrelativistic energies of the particles ($E \ll Mc^2 = 0.94$ Bev) has given a satisfactory quantitative description of the experiments on the scattering and photoproduction of π mesons and the right order of magnitude for the magnetic moments of the proton and neutron.[2]

These results of the nonrelativistic theory give us a right to think that the virtual cloud of π mesons is a reality. The nucleon, however, can dissociate not only into a nucleon and a π meson, but also into a K meson and a hyperon, a nucleon-antinucleon pair, etc.:

$$N \rightleftarrows N + \pi, \tag{1}$$

$$N \rightleftarrows Y + K, \tag{2}$$

$$N \rightleftarrows N + N + \tilde{N}. \tag{3}$$

Considerations analogous to those just given regarding process (1) lead to the conclusion that besides the pion cloud with the characteristic dimension $\hbar/m_\pi c$, there must also exist around a nucleon a cloud of virtual K mesons with the characteristic dimension $h/m_K c$ (m_K is the mass of the K meson; $m_K \approx M/2$),* and a cloud of virtual pairs $(N, \tilde{N})$ with the characteristic dimension $\hbar/Mc$ (M is the mass of the nucleon).

Figure 1 shows a perhaps somewhat naive picture of the structure of a physical nucleon, as it

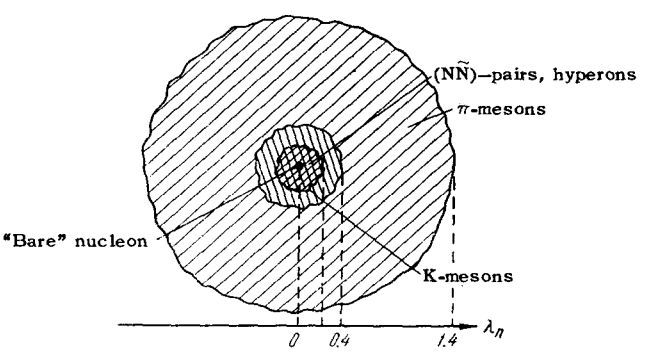

FIG. 1. The π-meson, K-meson, and other shells in the nucleon.

*The operator for emission of a meson is proportional to $1/\omega_k^{1/2}$; $\hbar\omega_k = [(\hbar ck)^2 + (\mu c^2)^2]^{1/2}$, and k is the wave vector of the meson.

*The coupling of the K mesons to the "bare" nucleon is evidently weaker than the coupling of the pions to the nucleon. Therefore the K-meson cloud is also less intense than the pion cloud (cf. reference 39).

follows from the idea of the possible virtual processes inside the nucleon.

This physical picture leads to the idea of the existence of two different regions inside the nucleon — an outer pion shell and a central part, or "core," where K mesons, nucleon-antinucleon pairs, and hyperons are of importance. The characteristic dimension of the "core" is $\sim \hbar/Mc = 2.1 \times 10^{-14}$ cm, which is several times smaller than the size of the pion shell.*

At present the information we have about the "core" of the nucleon is very slight. We can hope, however, that we do know much more about the pion shell of the nucleon. In any case it is clear that if present theoretical ideas are capable of describing even in very rough outline the structure of such "elementary" particles as the nucleon, then it must be true that charged virtual mesons produce a distribution of electric charge and current in the pion shell of the nucleon. In particular, these currents must also be the cause of the anomalous magnetic moments of nucleons.

Proceeding further, we shall examine the experimental arguments in favor of the picture of nucleon structure that has been described. We shall see that the mosaic of physical ideas, experimental data, and calculations is still far from fitting together into a harmonious and definitive picture; but we can console ourselves with the thought that as recently as about ten years ago the very word "structure" of the nucleon would have seemed criminal to the majority of physicists.

2. METHODS FOR STUDYING THE STRUCTURES OF PARTICLES

The best way to study the structure of an object is to see it. The small dimensions of the microscopic particles obviously exclude this possibility. There remains, however, something analogous; this is elastic scattering by the particle under study of some sort of rays with wavelength $\lambda\!\!\!^{-}$ smaller than the dimensions a of the particle.

By observing such scattering in an assembly of particles, we get an average optical image of the particle, from which, under certain conditions, we can get also a space-time picture of the structure of the particle in relation to the given type of rays. An example of this kind of measurements is the experiments on the scattering of electrons or γ-ray quanta by nucleons.

To obtain more and more detailed information on the structure of a particle, we must use shorter and shorter waves. If we confine ourselves to wavelengths $\lambda\!\!\!^{-}$ that are larger than the Compton wavelength $\hbar/\mu c$ of the lightest particles coupled to the nucleon (these particles are the π mesons), effects of the nuclear structure will not play any important role. For example, the scattering of light with wavelength $\lambda\!\!\!^{-} \gg \hbar/m_\pi c$ will give information only about the value of the total charge of the nucleon. For smaller values of $\lambda\!\!\!^{-}$ the scattering already depends on the anomalous magnetic moment of the nucleon, and for $\lambda\!\!\!^{-} < \hbar/m_\pi c$ the detailed dynamical structure of the nucleon takes on importance. In this case the scattering cross-section is decidedly different from that for scattering by a point particle.

It must be kept in mind that as the wavelength of the rays used to study the structure of a particle is made smaller new effects are sure to appear that complicate the simple picture of "seeing" the structure. These are, first, recoil effects, and second, inelastic processes. Let us consider each of them in turn.

A. The Effect of Recoil

If the wavelength $\lambda\!\!\!^{-}$ of the rays is smaller than $\hbar/Mc$, where M is the mass of the particle being studied, then in its interaction with the incident particles the particle under study has its motion considerably changed because of the momentum transferred to it. To get an idea of the important way this affects the optical image of the particle, let us suppose that the internal structure of the particle can be described by a wave function $\psi_1(\mathbf{k};\xi)$, where $\mathbf{k}$ is the energy-momentum vector of the particle before its interaction with the ray, and ξ denotes the internal coordinates of the particle. Furthermore let $\psi_2(\mathbf{k}';\xi)$ be the wave function after the interaction with the ray ($\mathbf{k}'$ is the energy-momentum vector after the interaction). The experimentally determined quantity (the form-factor of the particle) involves the product of $\psi_1(\mathbf{k};\xi)$ and $\psi_2(\mathbf{k}';\xi)$. Therefore the optical image is of necessity a superposition of the pictures of the initial and final states, which differ from each other in the directions and magnitudes of their Lorentz contractions.

From relativistic considerations we see that the Fourier component of the form-factor F is a function of $(\mathbf{k}'-\mathbf{k})^2 = \Delta\mathbf{k}^2 - \Delta\epsilon^2$ ($\Delta\mathbf{k} = \mathbf{k}'-\mathbf{k}$, $\Delta\epsilon = \epsilon'-\epsilon$, where $\mathbf{k}$ is the space and ϵ the

*Jastrow was evidently the first to obtain from an analysis of nucleon-nucleon scattering the conclusion that there exists a core of the nucleon – a region of a large repulsive potential.[3] One of us[4,5] arrived at the existence of a core of the nucleon from quite different considerations.

time part of the four-vector k), i.e.,

$$F = F(\Delta \mathbf{k}^2 - \Delta\epsilon^2). \quad (4)$$

In the center-of-mass system the energy transfer is $\Delta\epsilon = 0$, and the form-factor admits of interpretation as the image of a certain spatial distribution

$$\rho(\xi) = \int F(\Delta \mathbf{k}^2)\, e^{i\Delta \mathbf{k}\xi} d(\Delta \mathbf{k}). \quad (5)$$

This distribution, however, is a superposition of two distributions, that "before the experiment" and that "after the experiment." If we agree to regard such a generalized distribution as the image of the particle's structure, then with a sufficiently large number of acts of scattering (with "large statistics," as one usually says) and with a sufficiently short wavelength $\lambda\!\!\!^{-}$ it is possible in principle to get such an optical image of the particle as precisely as we wish.

B. Inelastic Processes

With decrease of the wavelength $\lambda\!\!\!^{-}$, i.e., with increase of the energy of the scattered particles, inelastic processes become more and more important. They play a particularly large role in the case of strong interactions. The experimental data available at present on the pion-nucleon and nucleon-nucleon interactions show that the interaction cross-sections do not fall off with increasing energy, but rather remain constant. This can be seen, for example, from Table I, which shows the experimental values, together with their statistical errors, of the cross-sections for inelastic interactions of protons and neutrons with iron nuclei at high energies.[56] The average energy for each interval in Table I has been calculated on the basis of the energy spectrum of the protons in the atmosphere. The measurements of Grigorov and his coworkers[6] and of Begzhanov et al.[7] also lead to similar conclusions. The tendencies in the case of the electromagnetic interactions are less obvious. At high energies, however, it is scarcely legitimate to treat electromagnetic interactions apart from other interactions, in particular from the interactions that lead to the production of μ mesons and neutrinos. Theoretical estimates show that at very high energies these processes become strong, in the sense that the cross sections become larger than $\pi\lambda\!\!\!^{-2}$ ($\lambda\!\!\!^{-}$ is the wavelength of the photon).[8]

It seems very probable that the constancy of the cross sections of inelastic processes at large energies is a general effect, and this fact may be of importance in principle for the spatio-temporal description of phenomena on a very small scale.

TABLE I

Energy range (Bev)	Average energy (Bev)	σ_{in} (n+Fe) ($\times 10^{24}$ cm^2)	σ_{in} (p+Fe) ($\times 10^{24}$ cm^2)
28—58	37	0.60 ± 0.04	0.59 ± 0.05
58—121	77	0.62 ± 0.05	0.61 ± 0.06
121—387	178	0.67 ± 0.13	0.79 ± 0.25
28—387	50	0.61 ± 0.03	0.61 ± 0.04

In fact, with increasing energy the number of possible channels for inelastic processes will increase; this means that with increasing energy the cross section for elastic nondiffractive scattering will go to zero. But just this elastic scattering is the source of information about the spatio-temporal structure of particles; meanwhile, with increasing energy the total elastic scattering will gradually come down to the diffraction scattering only, which is completely determined by the inelastic processes.

These considerations can be illustrated by the conclusions of the statistical theory of the multiple production of particles. According to this theory, for (π, p) collisions at E = 5 Bev the cross-section of elastic nondiffractive scattering is $\sigma_{nd} = 6 \times 10^{-3}\sigma_{in}$ (σ_{in} is the cross-section for the inelastic processes), and at E = 7 Bev, $\sigma_{nd} = 1.5 \times 10^{-3}\sigma_{in}$, whereas the cross section for the diffraction scattering is $\sigma_d = 0.3\,\sigma_{in}$.[9] Similarly, for (p, p) collisions $\sigma_{nd} = 5 \times 10^{-3}$, 1×10^{-3}, and 2.5×10^{-4} times σ_{in} at E = 5, 7, and 10 Bev, whereas $\sigma_d = 0.3\,\sigma_{in}$.

The constancy of the diffraction scattering possibly indicates that a certain small internal region of the particle scatters like a "black ball" of radius R. It is clear that in this case the maximum information that can be obtained from the scattering picture is limited to indications of the outer size of this "black ball." From this point of view the quantity R is the length that defines the genuine nonlocalness (cf. Fig. 2). This quantity is not a universal length, but depends on the type of interaction.*

At present we do not yet have an experimental proof of the existence of a "black" region inside

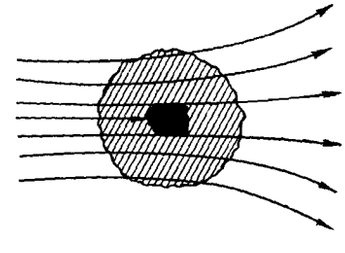

FIG. 2. "Gray" and "black" regions inside a nucleon. For $\lambda\!\!\!^{-} \to 0$ the elastic scattering becomes mainly diffraction scattering. The "black" region is the region of possible "nonlocal" behavior.

*We note that the size R of the "black ball," which defines the scale of the nonlocalness, can be introduced into the theory in a relativistically invariant way.[10]

TABLE II. Wavelength of various rays

Source of rays	Nature of rays	Wavelength in center-of-mass system of nucleon and scattered particle (ray), in units $\lambda = 10^{-13}$ cm
Berkeley betatron, 6 Bev	Protons (6.15 Bev)	0.12
	Pions (5 Bev)	0.13
Proton synchrotron of Joint Institute for Nuclear Research	Protons (10 Bev)	0.09
	Pions (8 Bev)	0.10
	Protons (50 Bev)	0.04
Proton synchrotron, 50 Bev	Pions (50 Bev)	0.04
Linear accelerator for electrons at Stanford	Electrons (1 Bev)	0.35
Head-on collisions of proton beams at 10 Bev (future possibility)	Protons against protons at 10 Bev	0.018
Head-on collisions of protons and electrons at 10 Bev (future possibility)	Protons against electrons at 10 Bev	0.019
Head-on collisions of electrons at 500 Mev (future possibility)	Electrons against electrons at 500 Mev	0.4

the nucleon. Analysis of the experimental data on (π, p) and (p, p) scattering shows, however, that there is in fact a tendency for "blackness" to appear in the central region of a nucleon, whereas the peripheral regions of the nucleon remain semitransparent ("gray").[10-14] If the scattering in these regions is also purely diffraction scattering, i.e., if $\sigma_{nd} \cong 0$, it can nevertheless be used to obtain information about the distribution of the absorption of π mesons or nucleons inside the nucleon, if these particles have sufficiently small wavelengths. Thus the study of the diffraction scattering of particles is also to be regarded as a way of studying the structure of the nucleon. In this connection we must also emphasize the importance in principle of further measurements of the interaction cross sections of ultrahigh-energy cosmic-ray particles colliding with various nuclei. By using the optical model one can get from these measurements the cross-sections for the interactions of the elementary particles at ultrahigh energies.[7,15]

C. Other Methods for Studying the Structure of Nucleons

In addition to the information from scattering processes, some data on the structure of nucleons are given by the study of bound states: the hyperfine splitting of the hydrogen lines, and the spectra of μ-mesonic atoms.[16] All these methods, however, give only rough average quantities characterizing the structure of nucleons, which do not compare in accuracy with the results achieved in experiments on the scattering of fast particles (electrons, π mesons, nucleons).

Therefore in concluding this section it is appropriate to indicate the wavelengths that are not at the disposal of experimenters, and also some possibilities for the future. These data are shown in Table II.*

3. THE ELECTROMAGNETIC STRUCTURE OF THE NUCLEON

The hypothesis of the existence of a cloud of charged mesons in a nucleon makes it extremely interesting to study the scattering of fast electrons by nucleons.†

We can make a theoretical calculation of the electric charge density $\rho_\pi(r)$ and the magnetic moment density $\mathfrak{M}_\pi(r)$ of the pion cloud in a nucleon by using the Chew-Low theory. In this theory, the nucleon is regarded as an extended source of the meson field. Furthermore it is taken to be infinitely heavy, so that recoils in virtual processes are neglected.

The behavior of the nucleon as an extended source of the meson field can be thought of as the result of the production, in the central region of the nucleon, of pairs of nucleons, antinucleons, and hyperons. In the first nonvanishing approximation Salzman[18] found that

*For reference we give a convenient formula for calculating the wavelength λ of a beam particle in the center-of-mass system:

$$\lambda = \lambda_0 \frac{V\sqrt{1-V^2}}{V\sqrt{T_2(T_2+2M)} - V(T_2+M)},$$

where $V = \{\sqrt{T_2(T_2+2M)} - \sqrt{T_1(T_1+2)}\}/(T_2+T_1+M+1)$; T_2 and T_1 are the respective kinetic energies of the beam particle and the particle regarded as the target, in the laboratory coordinate system; M is the mass of the beam particle. T_2, T_1, and M are expressed in units of the mass of the target particle; $\lambda_0 = \hbar/mc$ is the Compton wavelength of the target particle.

†This problem was first suggested in a dissertation by Saak'yan.[17]

$$\rho_\pi(r) = -\frac{4e\tau_3}{(2\pi)^5}\left(\frac{f}{\mu}\right)^2 \times \int \frac{v(k)\,v(k')\,(\mathbf{kk}')}{\omega(k)\,\omega(k')\,[\omega(k)+\omega(k')]} e^{i(\mathbf{k}-\mathbf{k}')\mathbf{r}} d^3(kk'), \quad (6)$$

$$\mathfrak{M}_\pi(r) = -\frac{2ie\tau_3}{(2\pi)^5}\left(\frac{f}{\mu}\right)^2 \times \int \frac{v(k)\,v(k')\,(\mathbf{k}\sigma)}{\omega^2(k)\,\omega^2(k')} \mathbf{r}\times[\mathbf{k}\times\mathbf{k}']\, e^{i(\mathbf{k}-\mathbf{k}')\mathbf{r}} d^3(kk'), \quad (7)$$

where $\omega(k) = (k^2+\mu^2)^{1/2}$, $\mu = m_\pi c/\hbar$, and $v(k)$ is a cutoff function that describes the source distribution for the π-meson field:

$$S(r) = \frac{1}{(2\pi)^3}\int v(k)\, e^{i\mathbf{kr}} d^3k. \quad (8)$$

The form of the function $S(r)$ for large values of r ($r > \hbar/m_\pi c$) has little effect on the results of the theory, since the source density that it describes is much smaller for $r > \hbar/m_\pi c$ than in the central regions of the nucleon. To a sufficient degree of accuracy we can set $S(r) \cong 0$ for $r > \hbar/m_\pi c$. (Cf. Gauss's theorem in electromagnetic theory.)

For $\xi = r/(\hbar/m_\pi c) > 1$ the charge density (6), whatever our choice of the shape-function $v(k)$, can be rewritten in the form

$$\rho_\pi(r) = -\tau_3 e\mu^3 f^2 \frac{2}{(2\pi)^{3/2}}\frac{e^{-2\xi}}{\xi^2} \times\left\{\frac{1}{\sqrt{2\xi+4}} + \frac{4}{\xi\sqrt{2\xi+5}} + \frac{13}{2\xi^2\sqrt{2\xi+6}} + \cdots\right\}. \quad (9)$$

Similarly, for $\xi > 1$ the expression (7) for the magnetic moment density can be rewritten in the form

$$\mathfrak{M}_\pi(r) = \tau_3 e\mu^2 c\,\frac{f^2}{4\pi}\,\mathbf{n}\times[\mathbf{n}\times\sigma]\,\frac{e^{-2\xi}}{\xi^2}\left\{1+\frac{2}{\xi}+\frac{1}{\xi^2}\right\}. \quad (10)$$

Here $\mathbf{n} = \mathbf{r}/r$.

It is very important that these asymptotic expressions do not depend on the shape of the source of the meson field [i.e., on the form of the function $v(k)$]. But, as will be seen from what follows (cf. Fig. 6), only a small part of the meson cloud is concentrated in the region $r > 1/\mu$ (this is, so to speak, the "stratosphere" of the nucleon). The expression (6) for $\rho_\pi(r)$ is easily brought into the form

$$\rho_\pi(r) = e\mu^3\tau_3\frac{4f^2}{(2\pi)^5}\int_0^\infty d\xi\left(\frac{dI}{dr}\right)^2, \quad (11)$$

where

$$I(r) = \int \frac{v(k)}{\omega(k)} e^{i\mathbf{kr}-\xi\omega(k)}\, d^3k; \quad (12)$$

and ξ is a new auxiliary variable.

Integrating over the angles in Eq. (12) and setting $v(k) \equiv V(\omega)$, we get

$$I(r) = \frac{2\pi}{ir}V\left(-\frac{d}{d\xi}\right)Q(\xi; r) + \text{comp. conj.} \quad (13)$$

$$Q(\xi; r) = \int_1^\infty e^{-\xi\omega + ir(\omega^2-1)^{1/2}} d\omega. \quad (14)$$

Then, setting $\omega = \cosh t$ and introducing the variable $\rho = (\xi^2 + r^2)^{1/2}$, we get

$$I(r) = -\frac{4\pi}{r}V\left(-\frac{d}{d\xi}\right)\frac{dK_0(\rho)}{dr}, \quad (15)$$

where $K_0(\rho)$ is the well known Bessel function.

Let us choose the cutoff form-factor $V(\omega)$ in the form

$$V(\omega) = e^{-\beta(\omega-1)}, \quad (16)$$

where β is a cutoff parameter. In this case the operator V in Eq. (15) is simply the displacement operator $\xi \to \xi + \beta$, and the charge density (11) can be written in the form

$$\rho_\pi(r) = e\mu^3\tau_3\frac{2f^2}{\pi^3}e^{2\beta}r^2\int_{\sqrt{\beta^2+r^2}}^\infty K_2^2(\rho)\frac{d\rho}{\rho^3\sqrt{\rho^2-r^2}}, \quad (17)$$

which is convenient for numerical calculations. In a similar way we can transform also the expression for the magnetic moment density, Eq. (7):

$$\mathfrak{M}_\pi(r) = e\mu^3 c\tau_3\frac{f^2}{2(2\pi)^3}e^{2\beta}\,\mathbf{r}\times[\sigma\times\mathbf{r}]\left\{\int_{\sqrt{\beta^2+r^2}}^\infty K_2(\rho)\frac{d\rho}{\rho\sqrt{\rho^2-r^2}}\right\}^2. \quad (18)$$

Generally speaking, the densities $\rho_\pi(r)$ and $\mathfrak{M}_\pi(r)$ depend strongly on the shape of the form-factor $V(\omega)$, and with our choice of $V(\omega)$, on the value of the cutoff parameter β. Figures 3 and 4 show as functions of the cutoff parameter β the values of the electric charge of the pion cloud

$$Q_\pi = \int \rho_\pi(r)\, d^3x \quad (19)$$

and its magnetic moment

$$\varkappa_\pi = \int \mathfrak{M}_\pi(r)\, d^3x, \quad (20)$$

and also the values of the corresponding mean square radii,

$$\langle r_e^2\rangle_\pi = \frac{1}{e}\int \rho_\pi(r)\, r^2\, d^3x \quad (21)$$

and

$$\langle r_m^2\rangle_\pi = \frac{0.6}{\varkappa}\int \mathfrak{M}_\pi(r)\, r^2\, d^3x. \quad (22)$$

Here $e = 1$ is the charge of the proton, and $\kappa = 1.85\,\hbar/2Mc$ is the anomalous magnetic moment of the proton. [The coefficient 0.6 is introduced to make the value of $\langle r_m^2\rangle_\pi$ agree with Eq. (30); see the further argument. Cf. also reference 18.]

It can be seen from these diagrams that the charge and the magnetic moment are very sensi-

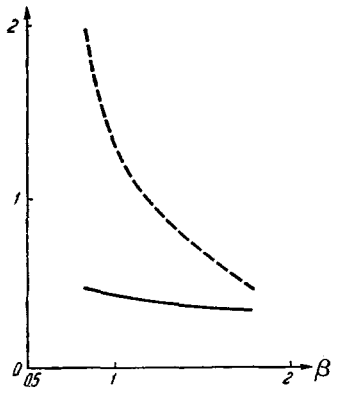

FIG. 3. Dashed line – dependence of the electric charge Q_π of the pion cloud around a nucleon on the value of the cutoff parameter β. Solid line – the electric mean-square radius $\langle r_e^2 \rangle_\pi$ as function of β.

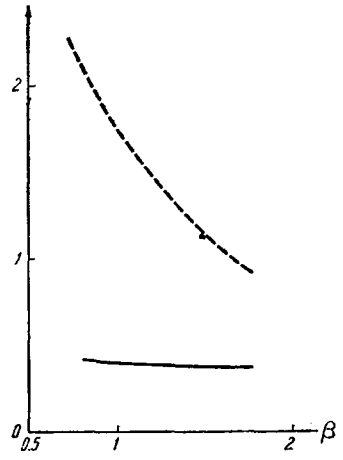

FIG. 4. Dashed line – dependence of the magnetic moment κ_π of the pion cloud on the value of the cutoff parameter β. Solid line – dependence on β of the magnetic mean-square radius $\langle r_m^2 \rangle_\pi$.

tive to the choice of β, whereas the values of the mean square radii are almost constant over a wide range of variation of the parameter β.

We shall choose the value of β so as to get the best agreement between the theoretical P phase shift for scattering of π mesons by nucleons and the experimental results in the low-energy region (as is well known, at low energies the P phase essentially determines the scattering). Calculations have shown that $\beta \cong 1/\eta$.

In this case (cf. Figs. 3 and 4).

$$\begin{aligned} &Q_\pi = 0.76 \text{ (the charge of the proton is taken as unity);} \\ &\varkappa_\pi = 1.2 \quad \text{(in units } e\hbar/2Mc\text{);} \\ &\langle r_e^2 \rangle_\pi = (0.62 \cdot 10^{-13} \text{ cm})^2; \\ &\langle r_m^2 \rangle_\pi = (0.62 \cdot 10^{-13} \text{ cm})^2. \end{aligned} \tag{23}$$

For the indicated choices of the form-factor and the cutoff parameter we have calculated the charge density per unit thickness of a spherical shell, $d_\pi(r) = 4\pi r^2 \rho_\pi(r)$, for a wide range of values of r.* The results of these calculations are shown in Table III.

*The calculated values of $\rho_\pi(r)$ differ decidedly from the values given in a paper by Zachariasen.[19] It has been stated in reference 20, however, that Zachariasen's results are erroneous.

TABLE III. Distribution of the electric charge of the pion cloud in the nucleon

$r \cdot m_\pi c/\hbar$	0	0.05	0.075	0.0875	0.1	0.125
$d_\pi(r)\left(\frac{\hbar}{m_\pi c}\right)\frac{1}{e}$	0	0.17	0.58	0.88	1.13	1.64
$r \cdot m_\pi c/\hbar$	0.15	0.2	0.3	0.4	0.5	0.6
$d_\pi(r)\left(\frac{\hbar}{m_\pi c}\right)\frac{1}{e}$	1.95	2.05	1.46	0.9	0.55	0.35
$r \cdot m_\pi c/\hbar$	1.0	1.5	2.0			
$d_\pi(r)\left(\frac{\hbar}{m_\pi c}\right)\frac{1}{e}$	0.146	0.082	0.0145			

As can be seen from this table, the electric charge contained in the peripheral region $r > \hbar/m_\pi c$ is insignificant in comparison with the charge of the pion cloud in the central regions of the nucleon.

There is now a possibility of checking the conclusions of the theory, owing to the operation of the electron linear accelerator in Stanford, where in recent years the Hofstadter group has been making measurements of the scattering of electrons with energies 100 to 650 Mev in hydrogen and deuterium. We shall not go into the details of these experiments, since they have been fully described in references 21 – 23; we shall just mention the most important points, which we shall need in our further discussion.

The basic idea of the experiments was to determine the deviations of the scattering from that of electrons of energy E colliding with point nucleons with anomalous magnetic moment κ. This scattering is described by the formula of Rosenbluth:[24]

$$\left[\frac{d\sigma}{d\Omega}\right]_{F=1} = \sigma_{NS}\left\{1 + \frac{\hbar^2 q^2}{4M^2c^2}\left[2(1+\varkappa)^2 \tan^2\frac{\theta}{2} + \varkappa^2\right]\right\}, \tag{24}$$

where

$$\sigma_{NS} = \left(q\,\frac{e^2\hbar c}{4E^2}\right)^2 \frac{\cos^2\frac{\theta}{2}}{\sin^4\frac{\theta}{2}} \tag{25}$$

is the Mott formula for the scattering of electrons by a point charge; $q = (2E/\hbar c)\sin(\theta/2)/\sqrt{1 + (2E/Mc^2)\sin^2(\theta/2)}$ is the momentum transferred; and θ is the angle of scattering of the electron in the laboratory coordinate system.

Inclusion of the effects of the distributions of the charge and magnetic moment in the nucleon leads to the appearance of form-factors $F_e(q)$

and $F_m(q)$ for the charge and magnetic moment, respectively; these quantities are functions of the momentum transfer q:

$$\frac{d\sigma}{d\Omega} = \sigma_{NS}\left\{F_e^2(q) + \frac{\hbar^2 q^2}{4M^2c^2} \times \left[2(F_e(q) + \varkappa F_m(q))^2 \tan^2\frac{\theta}{2} + \varkappa^2 F_m^2(q)\right]\right\}. \quad (26)$$

Under the limitations that we discussed earlier (cf. Sec. 2A), the form-factors are the Fourier transforms of the spatial distributions of the electric charge, $\rho(r)$, and of the magnetic moment, $\mathfrak{M}(r)$.

The analysis of the Hofstadter experiments is based on the Rosenbluth formula (24). This formula is only the first Born approximation in the scattering problem (Fig. 5a). The second approximation (cf. Fig. 5a') diverges for a nucleon with a point magnetic moment, i.e., for $F_m(q) = 1$.

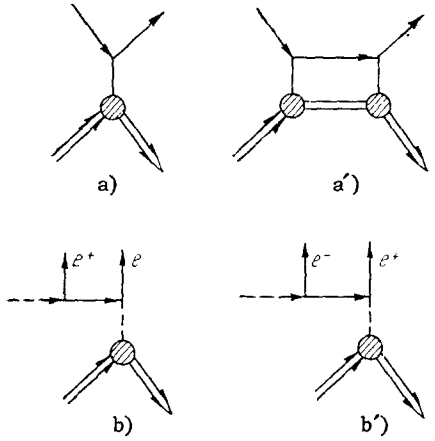

FIG. 5. Feynman diagrams for scattering of electrons, (a), (a'), and for the production of electron-positron pairs, (b), (b'), in the field of a nucleon. A solid double line is a proton, a solid single line an electron or positron, a wavy line a π-meson, and a dashed line a γ-ray quantum; the shaded areas indicate the form-factor.

The values of the form-factors $F_e(q)$ and $F_m(q)$ are determined from the experiments by use of the formula (26), and it cannot be asserted a priori that $F_e(q)$ and $F_m(q)$ differ appreciably from 1. Therefore, strictly speaking, to justify the interpretation of the results of Hofstadter it is necessary to show that the second Born approximation is much smaller than the first, when one uses the values of F_e and F_m obtained from Eq. (26). Calculations made recently by Drell and Fubini[36] have in fact shown that the contribution of the second Born approximation to the scattering cross-section does not exceed 1 percent right up to energies of the order of 1 Bev. In this way the application of the Rosenbluth formula (24) to the analysis of the Hofstadter experiments has been fully justified.

Let us now examine the main results of the experiments for the proton and for the neutron.

A. The Proton

Detailed summaries of the experimental results on the angular distributions of elastically scattered electrons are given in references 21–23. The experimental curves of the angular distributions lie considerably lower than is predicted by the formula for scattering by a point charge and point magnetic moment, Eq. (24).

The experimental and theoretical curves can be reconciled only if we assume that the scattering occurs by interaction with an extended electric charge and magnetic moment. The best agreement with experiment is obtained if for the proton we set

$$F_e(q) = F_m(q) \quad (27)$$

and choose the corresponding spatial distribution $\rho(r)$ [cf. Eq. (5)] in the form

$$\rho(r) = \frac{1}{8\pi a^3} e^{-r/a}; \qquad a = 2.3\cdot 10^{-14}\ \text{cm}, \quad (28)$$

that is, $a \sim \hbar/Mc$.

The way this formula fits into the theory will be considered later.

For small values of q the form-factors can be expanded in series

$$F_e(q) = 1 - \frac{1}{6}\langle r_e^2\rangle_p q^2 + \ldots, \quad (29)$$

$$F_m(q) = 1 - \frac{1}{6}\langle r_m^2\rangle_p q^2 + \ldots, \quad (30)$$

where

$$\langle r_e^2\rangle_p = \frac{1}{e}\int r^2 \rho(r)\, d^3x \quad (31)$$

is the mean square "electric" radius of the proton, e = 1 is the charge of the proton,

$$\langle r_m^2\rangle_p = \frac{1}{\varkappa}\int r^2 \mathfrak{M}(r)\, d^3x \quad (32)$$

is the mean square "magnetic" radius of the proton, and $\kappa = 1.85$ is the anomalous magnetic moment of the proton.

This definition of $\langle r_e^2\rangle$ and $\langle r_m^2\rangle$ is also adopted for the neutron (the anomalous magnetic moment of the neutron is $\kappa_n \approx -\kappa$).

According to Eq. (28) we have

$$\sqrt{\langle r_e^2\rangle_p} = (0.80 \pm 0.04)\cdot 10^{-13}\ \text{cm}. \quad (33)$$

The value of $(\langle r_m^2\rangle)^{1/2}$ is approximately the same.

In connection with the equality of the electric

and magnetic form-factors we must make the general remark that in actual fact it has been established only to an accuracy of about 20 percent.[22,25]

B. The Neutron

To study the electromagnetic structure of the neutron the Hofstadter group has made experiments on the scattering of fast electrons by deuterons. The results obtained from these experiments, and also from experiments on the scattering of slow, "thermal" neutrons by atoms (see further discussion), were completely unexpected, even paradoxical.

It was found that the best agreement between the theoretically calculated angular distribution of the electrons elastically scattered by deuterons is obtained if one assumes that the spatial distributions of the magnetic moments of the proton and neutron are the same,

$$\left.\begin{aligned} F_m(q) \equiv F_{m\mathrm{p}}(q) = F_{m\mathrm{n}}(q), \\ \langle r_m^2\rangle_{\mathrm{p}} = \langle r_m^2\rangle_{\mathrm{n}}, \end{aligned}\right\} \tag{34}$$

and the electric form-factor of the neutron is identically zero. This last fact means that the neutron, unlike the proton, has a very small electrical radius:

$$\langle r_e^2\rangle_{\mathrm{n}} \cong 0. \tag{35}$$

Information about the electrical structure of the neutron can also be obtained from experiments on the inelastic scattering of electrons by deuterons.

Since the deuteron is a weakly bound system, when the momentum transfer is large the proton and neutron can with great accuracy be regarded as independent. In this case the differential cross section for the scattering of electrons by the deuteron, $(d\sigma/d\Omega)_d$, is nearly equal to the sum of the differential cross sections for scattering by the proton and the neutron:

$$\left(\frac{d\sigma(\theta)}{d\Omega}\right)_d = (1+\Delta)\left[\left(\frac{d\sigma(\theta)}{d\Omega}\right)_{\mathrm{n}} + \left(\frac{d\sigma(\theta)}{d\Omega}\right)_{\mathrm{p}}\right], \tag{36}$$

where Δ is a correction of the order of a few percent, which allows for the kinetic effects of the motion of the nucleons in the deuteron, the interaction of the nucleons in the final state, and so on.[23,26]

Using the experimental values of $(d\sigma/d\Omega)_d$ and $(d\sigma/d\Omega)_p$ and taking the magnetic form-factors for the proton and neutron to be equal, Hofstadter got good agreement between the theoretically calculated cross section $(d\sigma/d\Omega)_n$ and experiment when the electric form-factor $F_{en}(q)$ was taken to be zero.

Thus two independent experiments — elastic and inelastic (ed) scattering — lead to the same conclusion about the distribution of the charges and currents in the neutron. The result about the smallness of the electrical radius of the neutron is also confirmed by experiments on the scattering of very slow, "thermal" neutrons by atoms.* These experiments require enormous precision, since a slow neutron is scattered both by the nucleus of the atom and by its electrons. The most accurate results in these experiments have been obtained by Havens, Rabi, and Rainwater.[27]

In this case the scattering amplitude can be written in the form $a_t = a_n + Za_e$, where a_n is the amplitude for scattering of the neutron by the nucleus, a_e is the amplitude for scattering by an electron, and Z is the number of electrons in the atom. It was found that $a_n \sim 10^{-12}$ cm, and $a_e \sim 1.5 \times 10^{-16}$ cm. It can be seen from these numbers that the cross-section of an atom with large Z differs from the cross section of the nucleus by only a few percent. The electron-nucleon interaction at low energies is expressed in terms of the value of the effective potential V_0, which is connected with the scattering amplitude by the relation

$$V_0\left(\frac{e^2}{m_e c^2}\right)^3 = \frac{3\hbar^2}{2M} a_e. \tag{37}$$

The calculation of V_0 according to relativistic theory gives the expression

$$V_0 = 3e\left(\frac{m_e c^2}{e^2}\right)^3 \left[\langle r_e^2\rangle_{\mathrm{n}} + \frac{\hbar}{2Mc}\varkappa_{\mathrm{n}}\right]. \tag{38}$$

As can be seen, V_0 consists of two parts: the first is due to the distribution of electric charge in the neutron (the part proportional to $\langle r_e^2\rangle_n$), and the second is determined by the value of the anomalous magnetic moment κ_n.

The experimental value of V_0 is $-(3860 \pm 370)$ ev, and the contribution from the magnetic moment of the neutron, $\kappa_n = -1.91$, is -4080 ev. Thus the part assignable to the electric interaction is (30 ± 200) ev. The corresponding value of the "electrical" radius of the neutron, permitted by the experimental error, cannot exceed 10 percent of the "electrical" radius of the proton:

$$\sqrt{\langle r_e^2\rangle_{\mathrm{n}}} \leqslant 0.1 \cdot \sqrt{\langle r_e^2\rangle_{\mathrm{p}}}. \tag{39}$$

Thus the analysis of the experimental data on the neutron seems to be in disagreement with the pion model, according to which, from considerations of the charge-independence of the interaction

*In this work one uses the atoms of the noble gases, with the magnetic moment of the electrons equal to zero, so as to eliminate the additional magnetic interaction with the neutron.

of π mesons with nucleons, the charge of the π-meson cloud in the neutron should be equal and opposite to that of the cloud in the proton,

$$\rho_{\pi p}(r) = -\rho_{\pi n}(r) \tag{40}$$

and consequently the mean square radii of these distributions should also be equal.

This is commonly regarded as a paradox in the results of the experiments on electron-neutron scattering.

As will be shown in our further discussion, this paradox is only an apparent one. It rests on an unjustified application of the elementary Yukawa theory to the central regions of the nucleon.

4. CRITICAL REMARKS AND ANALYSIS OF THE HOFSTADTER EXPERIMENTS

The disagreement that has appeared between the theory and the experimental data on the distribution of charge in the neutron forces us to make a more detailed analysis of all the conditions of the experiments and of all the theoretical assumptions underlying the studies of the scattering of electrons by nucleons.

A. The Limits of Electrodynamics

At Stanford they like to call attention to the fact that the basis of the theoretical analysis of the scattering of electrons by nucleons is the assumption that electrodynamics can be applied down to extremely small distances. Does a "break-down" of electrodynamics suddenly occur? The latest experimental work of Panofsky and Richter[25] and theoretical studies by Drell[28] are directed toward the answering of this question.

In the case of scattering of electrons by protons we could assume that all or a large part of the observed departure from point behavior of the nucleon is due not to a structure of the nucleon, but to a break-down of electrodynamics in regions of the size Λ_γ. The only conclusion that can be reached so far on this assumption is that if such a violation of electrodynamics actually occurs, then

$$\Lambda_\gamma \leqslant 0.3 \cdot 10^{-13} \text{ cm}.$$

In this connection there are also interesting possibilities in the study of the process of photoelectric pair production, $\gamma + p \rightarrow p + e^+ + e^-$ (cf. Figs. 5,b and 5,b'). In this case one studies deviations in the interaction of the electron with the photon. The accuracy of the experiments made so far gives a still higher limit for possible departures from the known laws of electrodynamics:

$$\Lambda_e \leqslant 0.6 \cdot 10^{-13} \text{ cm}.$$

Theoretically we can expect a break-down of electrodynamics through the involvement of μ mesons and neutrinos (for example, $e + e \rightarrow \mu + \mu$; $\gamma + e \rightarrow \mu + \nu + \nu'$) in spatial regions $\lambda\!\!\!^{-} < 10^{-16}$ cm. The study of such small spatial regions is far beyond the experimental possibilities now in prospect (cf. Table II).

Thus there are at present no experimental data on which to base an assumption that the phenomena we are discussing here could be affected to an important extent by departures from the laws of quantum electrodynamics.

B. The Role of Inelastic Processes

Along with the elastic process of scattering of electrons by nucleons there also occur inelastic processes; for example, for protons we have the reactions

$$e + p \rightarrow e + p + \gamma \quad \text{(deceleration radiation)} \tag{41}$$

$$e + p \rightarrow e + p + e^+ + e^- \quad \text{(pair production)} \tag{42}$$

$$e + p \rightarrow \left\{ \begin{matrix} e + n + \pi^+ \\ e + p + \pi^0 \end{matrix} \right\} \quad \text{(meson production)} \tag{43}$$

In principle these inelastic processes could make a contribution to the elastic scattering owing to the occurrence of diffraction scattering. In all these processes, however, the number of modes involved is large, and the phase shifts themselves are small. In such cases the inelastic scattering must be larger than the elastic by a large factor, if the diffraction scattering is to be appreciable. In fact, the cross section for elastic scattering is given by

$$\sigma_{el} = \sum_l \frac{\pi(2l+1)}{k^2} |1 - \beta_l e^{2i\delta_l}|^2$$

$$= \sum_e \frac{\pi(2l+1)}{k^2} [4\beta_l \sin^2 \delta_l + (1-\beta_l)^2]. \tag{44}$$

where the notations are the usual ones. The cross section for inelastic processes is

$$\sigma_{in} = \sum_l \frac{\pi(2l+1)}{k^2}(1 - \beta_l^2). \tag{45}$$

If the phase shifts for the inelastic process are small, i.e., if

$$\beta_l = 1 - \varepsilon_l; \qquad \varepsilon_l \ll 1,$$

then

$$\sigma_{in} = \frac{\pi}{k^2} \sum_l (2l+1)\, 2\varepsilon_l + O(\varepsilon_l^2), \tag{46}$$

$$\sigma_d = \frac{\pi}{k^2} \sum_l (2l+1)\{4\delta_l^2 + \varepsilon_l^2\}. \tag{47}$$

For the inelastic process to make an appreciable contribution to the elastic scattering, we must have $\epsilon_l \sim \delta_l$. Then

$$\sigma_{in} \sim \bar{a\varepsilon}; \quad \sigma_d = \bar{a\varepsilon}^2,$$

that is,

$$\frac{\sigma_{in}}{\sigma_{el}} \sim \frac{1}{\varepsilon} \quad \text{or} \quad \sigma_{in} \gg \sigma_{el}. \tag{48}$$

This is the condition to which we referred.

Estimates we have made on the basis of this inequality have shown that the diffraction scattering caused by pion production [reaction (43)] is of no importance. The same is evidently true for the processes (41) and (42). Deceleration radiation occurs mainly in the region of small angles, and it can scarcely be expected that it could give appreciable diffraction effects at scattering angles $> 30°$, where Hofstadter's measurements were made (cf. reference 29). The cross-section for pair production is smaller than that for deceleration radiation by about two orders of magnitude ($\sim e^2/\hbar c$).

C. Analysis of the Scattering of Electrons by Protons and Neutrons

It is usually stated emphatically that when one comes to speak of the distributions of electric charge and magnetic moment the meson theory is in decided contradiction with experiment. This assertion seems, however, to be too categorical.

In fact, one compares the distributions (6) and (7) with experiment. But these distributions have been obtained for the meson field produced by an infinitely heavy nucleon, and are valid only in the peripheral regions of the nucleon ($r > \hbar/m_\pi c$).

There are no grounds for hoping that these distributions will be valid over the entire range of values of r; on the contrary, we must expect considerable departures from them in regions $r < \hbar/m_\pi c$ (i.e., for momenta $q > m_\pi c$), where, in addition to recoil effects, there should be manifestations of the properties of the internal regions of the nucleon.

It seems more consistent to write the distributions $\rho_N(r)$ of the electric charge of the nucleon and $\mathfrak{M}_N(r)$ of its magnetic moment in the form of sums

$$\rho_N(r) = \tau_3 \rho_\pi(r) + \rho_{kN}(r), \tag{49}$$

$$\mathfrak{M}_N(r) = \tau_3 \mathfrak{M}_\pi(r) + \mathfrak{M}_{kN}(r), \tag{50}$$

where $\rho_{kN}(r)$ and $\mathfrak{M}_{kN}(r)$ denote the densities of electric charge and magnetic moment concentrated in the central part of the nucleon and caused by nucleon-antinucleon pairs, "strange" particles (charge and magnetic moment of the core of the nucleon), and also by two-pion, three-pion, and still more highly excited pion states. At present we know very little about these states and shall for the present ascribe them also to the core of the nucleon.

It is natural to expect that $\rho_{kN}(r)$ and $\mathfrak{M}_{kN}(r)$ will fall off with increasing r more rapidly than do $\rho_\pi(r)$ and $\mathfrak{M}_\pi(r)$.

Let us now consider the electrical radius of the nucleon in more detail. In accordance with the definitions (31) and (49),

$$\langle r_e^2 \rangle_N = \langle r_e^2 \rangle_{kN} + \tau_3 \langle r_e^2 \rangle_\pi, \tag{51}$$

where $\langle r_e^2 \rangle_{kN}$ is the mean square radius of the nucleon core. Regarding the isotopic symmetry of these expressions see Sec. 6B.

Setting

$$\rho_{kN}(r) = Q_{kN} \rho_c(r), \tag{52}$$

where Q_{kN} is the total charge of the core, and defining

$$\langle r_e^2 \rangle_c = \frac{1}{e} \int r^2 \rho_c(r)\, d^3x, \tag{53}$$

we can rewrite Eq. (51) in the form

$$\langle r_e^2 \rangle_N = Q_{kN} \langle r_e^2 \rangle_c + \tau_3 \langle r_e^2 \rangle_\pi. \tag{54}$$

It is known from experiment that the electrical radius of the neutron is very small, $\langle r_e^2 \rangle_n \approx 0$. It follows from this that

$$\langle r_e^2 \rangle_c = \frac{1}{Q_{kn}} \langle r_e^2 \rangle_\pi, \tag{55}$$

$$\langle r_e^2 \rangle_p = \langle r_e^2 \rangle_c. \tag{56}$$

Using the numerical values (23), we find that

$$\left.\begin{aligned} Q_{kn} &= +0.76; \\ \langle r_e^2 \rangle_p &= (0.7 \cdot 10^{-13}\ \text{cm})^2. \end{aligned}\right\} \tag{57}$$

Thus, setting the electrical radius of the neutron equal to zero we get a prediction of the electrical radius of the proton that is very close to the experimental value [cf. Eq. (33)].

The shape of the charge distribution in the core is still rather arbitrary (since only the integral quantities Q_{kN} and $\langle r_e^2 \rangle_c$ are known). For definiteness we choose $\rho_c(r)$ in the form

$$\rho_c(r) = \frac{e}{8\pi a^3} e^{-\frac{r}{a}}. \tag{58}$$

In this case, as can be verified easily,

$$\langle r_e^2 \rangle_c = 12a^2. \tag{59}$$

Now, in order to get $\langle r_e^2 \rangle_c = (0.7 \times 10^{-13}\ \text{cm})^2$, we must choose

$$a = \frac{1}{7} \frac{h}{m_\pi c} \approx \frac{\hbar}{Mc} = 2 \cdot 10^{-14}\ \text{cm}. \tag{60}$$

Thus Eq. (58) is an example of a core that is characterized by a small length a and at the same time has a large mean square radius.

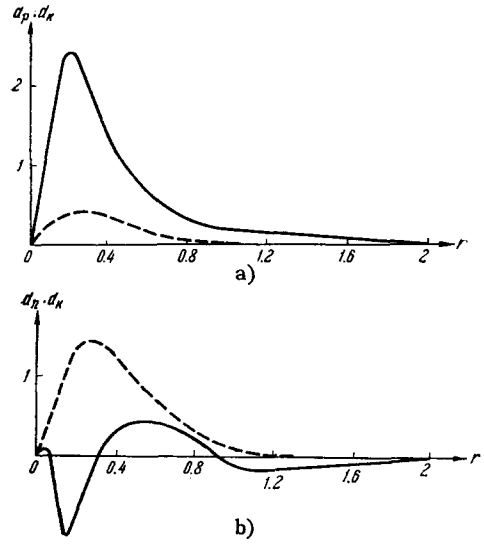

FIG. 6. Electromagnetic structure of nucleons. a – structure of the proton; b – structure of the neutron. The solid curves show the electric charge distributions in the proton and neutron; the dashed curves are the corresponding electric charge distributions in the cores of the proton and neutron.

Figures 6a and 6b show curves of the charge-density distributions in the proton and neutron and in their cores: $d_p(r) = d_\pi(r) + d_{kp}(r)$; $d_n(r) = -d_\pi(r) + d_{kn}(r)$, and $d_{kp}(r) = Q_{kp}d_c(r)$; $d_{kn}(r) = Q_{kn}d_c(r)$.

The curve $d_p(r)$ for the proton practically coincides with the curve obtained from the analysis of the experimental data in Hofstadter's papers.[21-23] As for the charge density in the neutron, it is seen that it oscillates around zero, and this explains the small electrical radius of the neutron.

In Figs. 6a and 6b a vertical line separates the region of the one-pion "atmosphere" of the nucleon from the region in which the charges in the core are involved to a considerable extent. As can be seen, in the one-pion region $r > \hbar/m_\pi c$. The region in which the asymptotic expansions (9) and (10) are valid, with the use of one or two terms, contains an extremely small number of mesons and belongs, figuratively speaking, to the "stratosphere" of the nucleon.

The magnetic structure of nucleons can also be treated in a similar way. We choose the distribution of magnetic moment in the core of the nucleon in exponential form

$$\mathfrak{M}_c(r) = \frac{\varkappa}{8\pi a^3} e^{-\frac{r}{a}} \qquad (61)$$

and take for a the value (60); from the condition $\kappa_p = -\kappa_n = 1.85\, e\hbar/2Mc$ we then get for the mean square magnetic radii of the proton and neutron the values

$$\langle r_m^2\rangle_p = \langle r_m^2\rangle_n = (0.7\cdot 10^{-13}\ \text{cm})^2, \qquad (62)$$

which are in good agreement with the experimental values found by Hofstadter.

Thus by assuming that a core exists in the nucleon, we can correlate the whole body of experimental data on the scattering of fast electrons by protons and deuterons and of slow neutrons by atoms with the fundamental ideas of the present meson theory.

Furthermore, the distributions of charge and magnetic moment in the core are characterized by the small length $a \approx \hbar/Mc \ll \hbar/m_\pi c$.

5. SOME EFFECTS OF THE STRUCTURE OF NUCLEONS

In this section we shall consider two more questions connected with the electromagnetic structure of the nucleon. These are the effect of the polarizability of the meson cloud in the nucleon, and the problem of the electromagnetic mass of the nucleons.

A. The Electric Polarizability of the Meson Cloud in the Nucleon

In determining the properties of the electromagnetic structure of the nucleon it is extremely important to consider, besides the scattering of fast electrons, other effects in which the electromagnetic structure of the nucleon can manifest itself. One of these effects is the scattering of slow nucleons in an inhomogeneous electric field, which produces a relative displacement of the clouds of charges of different signs in the nucleon and makes it into an electric dipole with the induced moment $\mathbf{p} = \alpha\mathbf{E}$. The electric polarizability of the charges in a nucleon can manifest itself in the Compton effect and in the photoproduction of pions from nucleons,[30] and also in the scattering of slow neutrons by nuclei.[31-33]

In the first approximation of the Chew theory (Fig. 7)

$$\alpha = \frac{2}{3\pi} e^2 f^2 \frac{1}{\mu^3} \int \frac{k^2}{\omega(k)} \left\{ v^2(k)\left[-27k^4 + 34k^2\omega^2(k)\right] + \left(\frac{dv(k)}{dk}\right)^2 4k^2\omega^4(k)\right\} dk. \qquad (63)$$

The same notations are used here as in Eqs. (6) and (7).

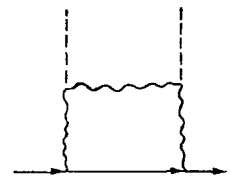

FIG. 7. Feynman diagram for the electric polarizability of the meson cloud in a nucleon. The solid line is the nucleon, the wavy line a pion, and the dashed lines are photons.

It is to be expected that, just as in the calculation of the magnetic moments of nucleons and of the interaction potential between a neutron and an electron, the higher terms of the expansion in powers of the coupling constant will not produce much change in the result.

From Eq. (63) one finds that

$$\alpha = 1.6 \cdot 10^{-42} \text{ cm}^3, \text{ if } v(k) = 1/\{1 + (k/5.6)^2\};$$
$$\alpha = 1.8 \cdot 10^{-42} \text{ cm}, \text{ if } v(k) = \exp\{-k^2/2 \cdot (5.6)^2\}.$$

These values are obtained with $f^2/\hbar c = 0.08$. Within a wide range of choices of the form of v (k) the results show very little sensitivity to this choice.

The calculated value of α is close to the value obtained by A. M. Baldin from an analysis of experiments on photoproduction and Compton effect in interactions of γ rays with nucleons[30]

$$4 \cdot 10^{-43} \text{ cm}^3 \leqslant \alpha \leqslant 1.4 \cdot 10^{-42} \text{ cm}^3,$$

but is much smaller than the value $\alpha \approx 8 \times 10^{-41}$ cm^3 obtained by Yu. A. Aleksandrov from experiments on the scattering of slow neutrons by heavy nuclei.[32] A more rigorous theoretical analysis of Aleksandrov's experiments is called for. It is possible that they involved effects of the interaction of the neutron with the electrons surrounding the heavy nucleus.

The experimental result confirming that the polarizability α of the neutron is not zero can be regarded as a direct proof of the existence of charged "clouds" in the neutron.

B. The Electromagnetic Masses of Nucleons and the Stability of the Proton

The small value of the neutron-proton mass difference [$\Delta (Mc^2) = 2.5$ electron masses] and the charge independence of the "nuclear interaction" of nucleons permit the assumption that this difference is of purely electromagnetic origin. Referring the reader to reference 59 for the details, we shall confine ourselves to an account of the qualitative side of the problem.

As a first approximation we can assume that the charge Q_{kN} and magnetic moment $\varkappa_{kN}$ of the core are concentrated at the center of the nucleon.

Then the electromagnetic energy of the nucleon can be written in the form

$$E_N = Q_{kN}\varphi_\pi(0) - \varkappa_{kN}\mathbf{H}_\pi(0), \tag{64}$$

where

$$\varphi_\pi(r) = \int \rho_\pi(r)\frac{d^3x}{r}; \quad \mathbf{H}_\pi(r) = \frac{1}{2c}\int [\mathbf{I}_\pi \times \mathbf{r}]\frac{d^3x}{r^3} \tag{65}$$

are the electrostatic potential and magnetic field produced at the center of the nucleon by the cloud of charged pions, and $\mathbf{I}_\pi$ is the electric current of the meson field.

Since

$$Q_{kn} + Q_{kp} = e \tag{66}$$

and

$$\varkappa_{kp} - \varkappa_{kn} = e\hbar/2Mc \tag{67}$$

(here the Dirac magnetic moment of the "bare" nucleon has also been included in the magnetic moment of the core), we have

$$\Delta(Mc^2) = E_n - E_p = \frac{e\hbar}{2Mc}H_\pi(0) - e\varphi_\pi(0). \tag{68}$$

As can be seen from this formula, the stability of the proton is entirely due to the energy of the interaction of the magnetic moment of the core of the proton with the currents of its pion cloud. The electrostatic energy of the proton, on the other hand, is larger than that of the neutron. When the numerical values of the parameters are substituted, Eq. (68) gives a value of the mass difference $\Delta (Mc^2)$ that agrees with experiment in order of magnitude; but the sign of $\Delta (Mc^2)$ is sensitive to the choice of the form of the cutoff form-factor v (k).

6. THEORETICAL ATTEMPTS AT AN INTERPRETATION OF THE ELECTROMAGNETIC STRUCTURE OF THE CENTRAL REGIONS OF NUCLEONS

In the preceding sections we have discussed in detail the electromagnetic properties of the peripheral regions in a nucleon and their theoretical interpretation. Let us now consider some theoretical attempts at an interpretation of the properties of the central regions of a nucleon.

A. The Influence of "Strange" Particles

Sandri,[37] and also independently one of us, have called attention to the fact that the dissociation of the nucleon into a hyperon and a K meson leads to the formation of a positively charged K-meson cloud in the case of the neutron as well as in that of the proton.

This effect must lead to an increase of $\langle r_e^2 \rangle_{kp}$ and to a decrease of $\langle r_e^2 \rangle_{kn}$, in accordance with the picture of the structure of the nucleon shown in Fig. 6.

In fact, according to the laws of conservation of strangeness and of the baryon number, the possible processes are

$$p \rightleftarrows \Lambda^0 + K^+; \quad \Xi^0 + K^0 + K^+; \quad \Xi^- + K^+ + K^+$$

and

$$n \rightleftarrows \Lambda^0 + K^0; \quad \Xi^0 + K^0 + K^0; \quad \Xi^- + K^0 + K^+;$$
$$\Sigma^0 + K^0; \quad \Sigma^- + K^+.$$

To calculate this effect we have used the first approximation of the Chew theory, and find that the mean square "electrical" radius of the neutron is given by*

$$\langle r_e^2\rangle_n \equiv \langle r_e^2\rangle_{n\,(\pi+k)} = \frac{e}{2\pi}\left(\frac{Mc^2}{e^2}\right)\left(\frac{f^2}{m_\pi}\right)\left\{5.98 + \left(\frac{g}{f}\right)^2 0.07\right\}, \tag{69}$$

i.e., $\langle r_e^2\rangle_n \cong 0$ if the coupling constant of the K^+ meson with the nucleon is $g^2/\hbar c \cong 8$. But in this case it is hard to explain the experiments on the scattering and photoproduction of K mesons. For more probable values of $g^2/\hbar c$, with either the scalar or the pseudoscalar type of theory, the contribution of the K mesons to $\langle r_e^2\rangle_n$ does not exceed the order of 10 percent.

Thus there are as yet no grounds for supposing that the strange particles are capable of causing any significant change in the distribution of charge in the central regions of the nucleon.

B. The Contribution of Nucleon-Antinucleon Pairs

I. E. Tamm has proposed an explanation of the zero electrical radius $\langle r_e^2\rangle_n$ of the neutron in terms of the dissociation of virtual π mesons into nucleon pairs.[38]

If a π meson dissociates into a nucleon-antinucleon pair, $\pi \rightleftarrows N + \tilde{N}$, the antinucleon so produced can annihilate with the original "bare" nucleon that is at the center of the physical nucleon, and the remaining nucleon is displaced relative to the previous center by a distance of the order of $\hbar/m_\pi c$. Thus the positive charge of the core of the neutron is smeared out over a region of radius about $\hbar/m_\pi c$. Figuratively speaking, the core and the π meson change places (Fig. 8). In this case the mean electric charge density in the neutron during its interaction with an electron, and consequently also the quantity $\langle r_e^2\rangle_n$, is close to zero. On the other hand, the smearing out of the neutral core of the proton over a region of radius about $\hbar/m_\pi c$ cannot cause much change in the value of $\langle r_e^2\rangle_p$.

This hypothesis, however, has not been confirmed by the calculations. Estimates show that

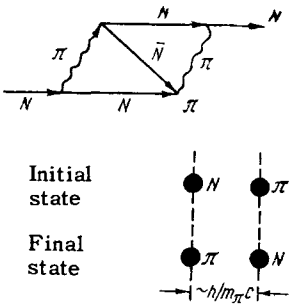

FIG. 8. Graphical illustration of the Tamm hypothesis.

the part played by $(N, \tilde{N})$ pairs is not large. The change of $\langle r_e^2\rangle_n$ caused by these pairs is negligibly small.[40]

The Tamm hypothesis also meets with the objection that it is hard to reconcile it with the uncertainty relation $\Delta p \cdot \Delta x \sim \hbar$. In fact, the uncertainty in the coordinate of the center of mass of the nucleon will be of the order of $\hbar/m_\pi c$ (this is just the uncertainty Δx of the point at which the nucleon-antinucleon pair is produced), and the uncertainty in the momentum is $\Delta p \sim \Delta E/c \sim Mc$. All of these remarks also apply to the hyperon pairs.

C. Application of Dispersion Relations

In recent times many attempts have been made to calculate the distributions of charge and magnetic moment in the nucleon, and also to take into account the contribution of the central regions, by using not only the Chew-Low method, but also the technique of dispersion relations.[40-43] We shall confine ourselves here to the discussion of some qualitative results. Let us consider the isotopic structure of the form-factors.

From considerations of charge symmetry it is natural to assume that the electric and magnetic form-factors of the nucleon can be represented in the form of combinations of isotopic vectors and scalars:

$$\left.\begin{aligned} eF_{ep}(q) &= G_e^s(q) + G_e^v(q); \quad \varkappa_p F_{mp}(q) = G_m^s(q) + G_m^v(q), \\ eF_{en}(q) &= G_e^s(q) - G_e^v(q); \quad \varkappa_n F_{mn}(q) = G_m^s(q) - G_m^v(q). \end{aligned}\right\} \tag{70}$$

Here G_e^V and G_m^V are the vector parts of the form-factors that determine the behavior of the electric and magnetic densities in the peripheral regions of the nucleon. In these regions the condition (40) holds.

Obviously

$$G_e^v(0) = \frac{e}{2}; \quad G_m^v(0) = \varkappa_p. \tag{71}$$

G_e^S and G_m^S are the scalar parts of the form-factors, which affect the properties of the central regions in the nucleon. These parts of the form-

*Since at present there are no experimental grounds for the introduction of a strong interaction of pions with K mesons,[39] which would considerably increase the spatial dimensions of the K-meson source, the form-factor for the K-meson source density has been taken the same as for the π-meson source.

factors satisfy the normalization conditions

$$G_e^s(0) = G_e^v(0) = \frac{e}{2}; \quad G_m^s(0) = 0. \tag{72}$$

Using the fact that $\kappa_p \cong -\kappa_n$, we get from the experimental relation $F_{mp} \cong F_{mn}$ the result

$$G_m^v \gg G_m^s, \tag{73}$$

i.e., the "magnetic form-factor" of the nucleon is mainly a vector in the isotopic space.

This fact obtained from experiment leads to the important conclusion that the magnetic structure of the nucleon is mainly due to a virtual process involving two mesons with opposite charges (Fig. 9a).*

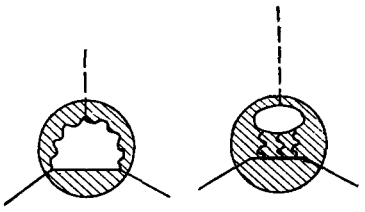

FIG. 9. a – Feynman diagram for the vector part of the electromagnetic form-factor of the nucleon; b – one of the Feynman diagrams for the scalar part of this form-factor. Solid line is the nucleon, wavy lines pions, dashed line photon.

This is understandable if we note the fact that a meson pair (π^+, π^-) forms a vector in the isotopic space, and that furthermore the intermediate state in this case is the vector state lowest in energy.[40,42] The next virtual state will be the state with four virtual mesons, and so on. It can be shown that the energy of the mesons in the main state with two intermediate mesons is $E_\pi < 1$ Bev.

As for the "electric form-factors" F_{ep} and F_{en}, they are determined to an important degree by the scalar form-factor G_e^s. The decisive process in this case is that with three virtual mesons. An example of one such virtual process is shown in Fig. 9b.

The calculation of the contribution from the process with three mesons is extremely complicated, and attempts at such a calculation have not led to any results so far.

Since, obviously, $\langle r_e^2\rangle_{pair} \lesssim 0.1 \cdot \langle r_e^2\rangle_p$ and $\langle r_e^2\rangle_{K\,meson} \lesssim 0.1 \cdot \langle r_e^2\rangle_p$, it is to be expected that

$$\langle r_e^2\rangle_{3\pi\ state} \leqslant 0.3\,\langle r_e^2\rangle_p. \tag{74}$$

All these results agree with the picture of the structure of the nucleon according to the static theory, as discussed earlier.

*In the terminology adopted in the theory of dispersion relations a state with one virtual π meson that makes an interaction before its absorption (cf. Fig. 9a) is called a two-pion state.

It must be noted that the analysis of the π-meson shell of the nucleon and the calculation of the form-factors G^S and G^V are carried out by means of so-called "truncated" dispersion relations, which at present are without foundation, since it has not been possible to justify the cutting off of the expansions used at any particular number of π mesons.

7. THE NUCLEAR STRUCTURE OF NUCLEONS

In the foregoing we have considered the problem of the structure of nucleons from the point of view of electromagnetic interactions.

Other sources of information on the structure of nucleons exist, however, in interactions of nucleons with each other, with pions, with K mes- s, ons, with antinucleons, and so on. In particular, several years ago the analysis of experiments on the scattering of nucleons by nucleons in the energy range of several hundred Mev led to the conclusion[3] that in these collisions the nucleon can be regarded as a "black ball" with radius $a \cong 5 \times 10^{-14}$ cm. On the other hand, the meson field in the nucleon extends to a much larger distance. This fact led one of the present authors to the idea of a nucleon consisting of a solid core – a region of extremely strong nuclear interactions – and a more weakly interacting π-meson shell.[5]

A. The Core of the Nucleon

At the present time our knowledge of the core of the nucleon is slight, and reduces essentially to the following facts:

1. In recent experiments on the interaction of nucleons of energy 9 Bev, accelerated in the proton synchrotron at the Joint Institute for Nuclear Research, with nuclei in a photographic emulsion, two essentially different types of collisions are being observed, with large and small multiplicity of production of secondary particles in a single act of nucleon-nucleon collision.[44]

In the majority of the collisions there is a large multiplicity of the secondary particles ($n \geq 3-4$). In this case the energy loss of the primary nucleon in the single act of nucleon-nucleon collision is 40 ± 10 percent of the initial energy. In the center-of-mass system the angular distribution of the particles produced in the collisions is nearly isotropic for $n > 3-4$ (Fig. 10). In a considerably smaller number of cases collisions are observed with a small intensity of secondary particles. The energy losses in these collisions are obviously also smaller than in collisions of the first type. The angular distribu-

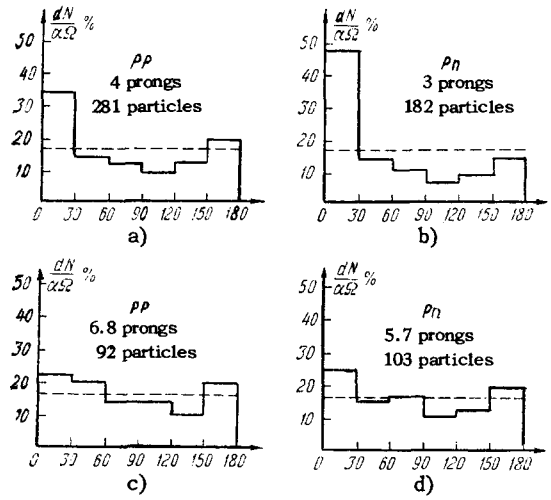

FIG. 10. Histograms of the distributions of numbers of charged particles produced in proton-proton and proton-neutron collisions at energy 9 Bev. Abscissas are values of the angle of emission of the particles in the center-of-mass system.[44]

tion of the emitted particles is decidedly anisotropic (in the center-of-mass system) (cf. Fig. 10).

Collisions of the first type (with large multiplicity) can be regarded as collisions of the cores of the nucleons. A large fraction of the collisions of the second type (with small multiplicity) can be regarded as collisions of the core of one nucleon with the peripheral shell of another nucleon.

It must be remarked, however, that at the present time such a division can be made only with great caution, since some of the stars of the second type may also be produced in collisions of the cores of nucleons, but with the production of a small number of particles. At present it is also not clear what part of the experimentally observed anisotropy of the angular distribution is due to the law of conservation of angular momentum in the core-core collisions.

A calculation of the energy loss and angular asymmetry (in the c.m. system) made on the assumption that about 80 percent of all collisions at energies $E \cong 10$ Bev are collisions between cores gives satisfactory agreement with experiment.[60]

In the laboratory coordinate system the particles produced in peripheral collisions must emerge at small angles. Table IV shows values of the ratio of the number of particles observed experimentally to emerge at angles $\theta \leq 10°$ to the number predicted according to the statistical theory of multiple production.[45]

It can be seen from this table that at small angles there is a large contribution by particles produced owing to a mechanism not described by

TABLE IV. Angular distribution of prongs from (N, N) collisions (laboratory system)

Range of angles	Number of particles, (Exptl.): (Calculated)
0°— 3°	2.2
0 — 5	1.9
0 —10	1.4

the statistical theory of multiple production. (Here again, however, no account has been taken of changes in the distribution that may be introduced by the law of conservation of angular momentum.)

2. The cross sections for the production of strange particles calculated by the statistical theory of multiple production can be reconciled with experiment only on the assumption that the K mesons are concentrated in a region $\sim \hbar/m_K c$ in the nucleon (m_K is the mass of the K meson).[39]

3. An optical analysis of the elastic scattering of nucleons and pions by nucleons at energies $E = 1 - 10$ Bev leads to the conclusion that there is a rapid rise of the absorption coefficient in a region $\sim \hbar/Mc$ (see below).

4. Comparison with experiment of numerous calculations made within the framework of the Chew-Low theory has shown that agreement with experiment can be obtained only by assuming that the size of the source of the pion field in the nucleon is $a \sim \hbar/Mc$. (From the mathematical point of view, in the Chew-Low theory this fact means a form-factor with cut-off frequency $\omega \sim \hbar/a$).

5. The analysis of the Hofstadter experiments and the (ne) interaction made above also leads to the conclusion that the central region of the nucleon has special properties.

6. Various types of meson theory lead to the qualitative result that there is a core in the nucleon (cf., e.g., reference 42).

Our knowledge about the core of the nucleon is at present confined essentially to these scanty indications.

B. The Optical Model of the Nucleon

The study of the structure of the nucleon by means of the scattering of nucleons, pions, and strange particles differs radically from the study by means of photons and electrons because of the largeness of the interaction.

In these cases the Born approximation is quite

useless; but only this approximation allows us to get the interaction-energy operator and the structural form-factors by a simple Fourier transformation of the amplitude of the scattered wave. In the general case no methods are known for solving the so-called "inverse problem," i.e., the problem of finding the law of interaction of the particles from the phases of the scattered waves.

The interesting and important studies made in this connection by I. M. Gel'fand,[48] Marchenko,[49] Krein,[50] and others[51] cannot be applied here, since in the high-energy region the concept of the interaction potential loses its meaning (see below).

The fact, however, that at high energies of the interacting particles the wavelength becomes much smaller than the dimensions of the nucleon (cf. Table II) permits us to expect that a quasiclassical approximation can be used. In this case the motion of a particle inside the nucleon can be regarded as occurring along a trajectory (a ray) in a medium with prescribed index of refraction $n = n(r)$ and absorption coefficient $k = k(r)$.

If the changes of these quantities in a wavelength $\lambda\!\!\!^{-}$ of the particle are small, the nucleon can be regarded as an optically inhomogeneous medium with smoothly varying optical constants, and the laws of geometrical optics can be applied to the scattering of the particles.

The problem can be further simplified, owing to the fact that at large energies of the pions or nucleons the cross-section σ_d for diffraction scattering is much larger than the cross-section σ_{nd} for nondiffractive scattering, so that the real part of the elastic-scattering amplitude is relatively small:

$$\operatorname{Re} F(\theta) \ll \operatorname{Im} F(\theta). \tag{75}$$

This means that the index of refraction of the nucleon is pure imaginary and reduces to the absorption coefficient. In this case the phases η_e of the scattered waves are also pure imaginary:[13]

$$n_e \ll k_e. \tag{76}$$

This enables us to determine the amplitude of the scattered wave

$$f(k;\theta) = \frac{\lambda\!\!\!^{-}}{2i}\sum_{e=0}^{\infty}(2l+1)(1-e^{ri\eta_e})P_e(\cos\theta) \tag{77}$$

(where θ is the angle of scattering) directly in terms of the cross-section for elastic scattering

$$f(k;\theta) \approx \left[\frac{d\sigma_d(k;\theta)}{d\Omega}\right]^{\frac{1}{2}} \tag{78}$$

and, by expanding this expression in terms of the Legendre polynomials $P_e(\cos\theta)$, to find the phases η_e:

$$\eta_{le} = -\frac{i}{2}\ln\left\{1-\frac{1}{\lambda\!\!\!^{-}}\int_0^{\infty}\sqrt{d\sigma_d(k;\theta)/d\Omega}\,P_e(\cos\theta)\sin\theta\,d\theta\right\}. \tag{79}$$

Calculations have shown that for pion-nucleon interactions the conditions (75) and (76) are satisfactorily fulfilled for energies $E > 1$ Bev.[10-14,52]

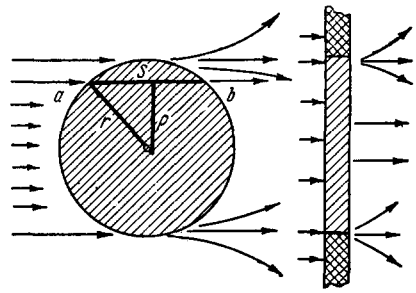

FIG. 11. S is the path of a pion inside the nucleon; $\rho \cong \lambda\!\!\!^{-} l$ is the impact parameter; r is the distance to the center of the nucleon. Mesons are absorbed along the length ab = S. The transparency is given by $D(\rho) = \exp\{-2\eta(\rho)\}$. Outside the nucleon $D(\rho) = 1$. The diffraction arising because of this limited transparency of the nucleon is precisely the same as the diffraction from an aperture in a screen, with transparency $\tilde{D}(\rho) = 1 - \exp\{-2\eta(\rho)\}$.

In the quasiclassical approximation the phase η_l corresponding to the impact parameter $\rho = \lambda\!\!\!^{-}\sqrt{l(l+\frac{1}{2})} \approx \lambda\!\!\!^{-} l$ is completely determined by the absorption of the pions on their paths through the nucleon (Fig. 11). Therefore, if we denote by $k(r)$ the absorption coefficient for a pion at the distance $r = (\rho^2 + s^2)^{1/2}$ from the center of the nucleon, we can write

$$\eta_l = \eta(\rho) = 2i\int_0^{\infty} k\left(\sqrt{\rho^2+s^2}\right)ds \tag{80}$$

or

$$\eta(\rho) = 2i\int_{\rho}^{\infty}\frac{k(r)\,dr}{\sqrt{r^2-\rho^2}}. \tag{81}$$

Knowing $\eta(\rho)$ from experiment, we can determine $k(r)$ (by a numerical method) for each value of the impact parameter. It has been found in practice that for energies of the order of several Bev it is enough to know 6 or 7 phases ($l = 0, 1, 2, \ldots$).

The absorption coefficient for pions calculated in this way is shown in Fig. 12 for pion energies $E = 1.3$ Bev and $E = 5$ Bev (cf. references 10 and 11). As can be seen, there is a tendency toward the appearance of "blackness" near the center of the nucleon. The mean square "pion" radius of the nucleus is found from these data to be

$$\langle r_\pi^2\rangle = (0.82\cdot 10^{-13}\ \text{cm})^2, \tag{82}$$

which agrees with the value of the "electromagnetic" radius of the proton, Eq. (33).

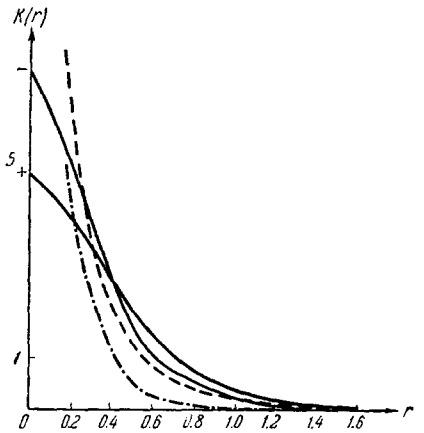

FIG. 12. Absorption coefficient for pions in a nucleon as function of the distance r from the center of the nucleon, k = k(r). The values of r are in units 10^{-13} cm, those of k(r). in units 10^{13} cm^{-1}. The solid curves are values of k(r) found from the extreme experimental values for E = 1.3 Bev. The dashed curve is the mean values of k(r) for E = 5 Bev. The dash-dot line is the function $k(r) = \sigma_{\pi\pi}\rho(r)$ constructed on the basis of theoretical values of the density $\rho(r)$.

It must be noted, however, that it can be seen from these data that in the central regions of the nucleon the conditions for the applicability of the optical model are poorly fulfilled. At large values of r ($r \gtrsim \hbar/m_\pi c$) the inaccuracy of the experimental data leads to a large spread of possible values of k(r), as can be seen from the curves of Fig. 12. Thus the most reliable values are those in the intermediate range of distances r.

TABLE V. Ratio of optical refraction and absorption coefficients for (pp) collisions

E (Bev)	1.5	2.24	2.75	4.40	6.15	9.0
$n(r)/k(r)$	1.2	1.2	0.95	0.51	0.1	0.05

For nucleon-nucleon collisions the validity of the conditions (75) and (76) begins at considerably higher energies than for the (πN) collisions. This can be seen from Table V, which shows values of the ratio of the coefficients n(r) and k(r) for energies E = 1 — 10 Bev, as calculated from experimental data. The conditions (75) and (76) are satisfied to sufficient accuracy only for energies E > 5 Bev. In papers by Huang Nien-Ning and one of the writers[13,14] a method is proposed for calculating the absorption coefficient k(r) and the index of refraction n(r) in terms of the relative coefficients $k = k(r)/k^*(r)$ and $n = n(r)/k^*(r)$, where the function $k^*(r)$ is determined from the known experimental data for E > 5 Bev. The calculations are also considerably simplified in this case.

Calculations have shown (cf. references 12 — 14) that the spatial shapes of k(r) and n(r) for nucleon-nucleon collisions are similar to those shown in Fig. 12 for the case of pion-nucleon collisions. The value of the mean square radius $\langle r^2 \rangle$ agrees with Eq. (82).

A knowledge of the absorption coefficient for pions in the pion shell of the nucleon enables us in principle to determine the cross-section $\sigma_{\pi\pi}$ for the interaction of pions. Let us examine the questions that arise in this connection.

C. The Pion-Pion Interaction

Pions can be regarded as particles consisting of virtual nucleon-antinucleon pairs. (Cf. reference 53, which also gives a detailed bibliography.)

On this basis the "structure" of the pion can be expressed by the symbolic formulas:

$$\pi^+ = p\tilde{n}; \quad \pi^- = \tilde{p}n; \quad \pi^0 = 2^{-\frac{1}{2}}(pn + \tilde{p}\tilde{n}); \tag{83}$$

and the hypothetical pion[54] by

$$\pi_0^0 = 2^{-\frac{1}{2}}(pn - \tilde{p}\tilde{n}). \tag{83'}$$

Here p, n are proton and neutron, and $\tilde{p}$ and $\tilde{n}$ are antiproton and antineutron.

This treatment of the pion as a compound particle allows us to regard the size a of the pion as the distance between the particles or antiparticles into which the pion virtually dissociates. Because of the strong interaction between nucleons it must be supposed that the cross section for pion-pion interaction is

$$\sigma_{\pi\pi} \cong \pi a^2. \tag{84}$$

We can estimate the distance a in its turn from the mass difference of the $\pi^\pm$ and π^0 mesons, which amounts to nine electron masses and is the difference of the electromagnetic energies of the charged and neutral pions. This difference is given by

$$\Delta E = \alpha \frac{e^2}{a} + \beta \left(\frac{e\hbar}{2Mc}\right)^2 \frac{\mathfrak{M}^2}{a^3}. \tag{85}$$

Here the first term is the electrostatic energy; the second term is the magnetic energy; the numbers α and β are of the order of unity; and $\mathfrak{M}$ is the total magnetic moment of the nucleon ($|\mathfrak{M}| \approx 2$). Setting $\Delta E = 9m_0c^2$, we find $a \approx 2\hbar/Mc$ and $\sigma_{\pi\pi} \approx 5 \times 10^{-27}$ cm^2. The absorption coefficient k(r) for pions inside a nucleon can be written approximately in the form

$$k(r) = \sigma_{\pi\pi}\, n(r), \tag{86}$$

where n(r) is the density of pions in the "atmos-

phere" of the nucleon. In the region of the one-pion state

$$n(r) \approx \frac{1}{e}\frac{3}{2}\rho(r), \tag{87}$$

where $\rho(r) = \rho_\pi(r) + \rho_K(r)$ is taken from Table III and Eq. (58) (the factor $^3/_2$ allows for the presence of neutral mesons).

Figure 12 includes the curve of $k(r)$ calculated from Eq. (86) for $\sigma_{\pi\pi} = 5 \times 10^{-27}$ cm^2. As can be seen from the diagram, there is agreement only in the most general aspects of the course of the curve.

Better agreement could, however, scarcely be expected, since in the region $r = 0.2$ to 1 the composition of the pion "atmosphere" does not reduce to the one-pion state, and we do not know the exact composition of $\rho_K(r)$.

In the region $r \cong 1$, on the other hand, as we have already remarked, the values of $k(r)$ obtained from the optical model are very doubtful.

Therefore more exact measurements of the diffraction scattering of pions by nucleons in the region of small angles are very important and promising as a means of determining the pion-pion interaction.*

8. THEORY OF THE OPTICAL MODEL OF THE NUCLEON

The optical theory of the scattering of particles by nucleons which we have considered is particularly simple and intuitive, but not without its naive aspects. In any case the model of the nucleon as a refracting and absorbing medium still stands in need of a serious theoretical and experimental foundation.

Two questions must be considered in this connection:

1. What are the conditions for the legitimacy of the optical model of the nucleon?

2. If the optical model is legitimate, then what are the conditions for the applicability of Eq. (81) for the calculation of the phases η_l?

Let us consider these questions.

A. The Equation for the Scattering of Pions by a Nucleon

At present we do not possess a general theory of the interaction of π mesons and nucleons. Therefore there is no entirely firm theoretical basis for an analysis of the significance of any sort of approximate method, in particular the optical model of the nucleon. Nevertheless some very general conclusions can be drawn about the conditions for the applicability of the optical model, or, in other words, of a complex interaction potential. For this purpose we write the Schrödinger equation for the system of pions and nucleons in momentum space in the form of a chain of relativistically invariant equations[55]

$$(E - H_0)\,\Phi_s = \sum_{s \neq s'} w_{ss'}\,\Phi_{s'}, \tag{88}$$

where $\Phi_S \equiv \Phi(\mathbf{k}_1; \mathbf{k}_2; \ldots; \mathbf{k}_S)$ is the wave function describing a possible real or virtual state of the particles involved in the interaction of a pion with a nucleon; $\mathbf{k}_S$ are the momenta of the particles; E is the total energy of the system; H_0 is the Hamiltonian of the noninteracting particles; and $w_{SS'}$ is the interaction operator describing the creation (or annihilation) of particles in the transition $s \to s'$.

In dealing with the optical model, out of all the functions Φ_S we concern ourselves with only the one function $\Phi_2 = \psi(\mathbf{k}; \mathbf{p})$ that describes the elastic scattering of a pion with momentum $\mathbf{k}_1 \equiv \mathbf{k}$ by a nucleon with momentum $\mathbf{k}_2 \equiv \mathbf{p}$.

To separate out this component $\Phi_2 = \psi$ we rewrite the system of equations (88) in the form

$$\left.\begin{aligned}(E - H_0)\,\psi &= \sum_{s' \neq 2} w_{2s'}\,\Phi_{s'},\\ (E - H_0)\,\Phi_{s'} &= \sum_{s' \neq 2} w_{s's''}\,\Phi_{s''} + w_{s'2}\,\psi,\end{aligned}\right\} \tag{89}$$

or, dividing the second equation by $(E - H_0)$ and introducing the "elementary scattering matrix" r, given by

$$r = \delta^+ (E - H_0)\, w \tag{90}$$

(for details see reference 55), we can rewrite the equations (89) in operator form

$$\left.\begin{aligned}(E - H_0)\,\psi &= w\Phi,\\ \Phi &= r\psi + r\Phi.\end{aligned}\right\} \tag{91}$$

From this we get by iteration the equation for the function ψ with which we are concerned:

$$(E - H_0)\,\psi = w\frac{r}{1-r}\psi + (wr^N\Phi)_{N\to\infty}. \tag{92}$$

If we assume that

a) all the diverging terms are excluded from this equation, and

b) the remainder term for $N \to \infty$ goes to zero (cf. reference 57), then this equation can be written in the form

$$\{E - E(\mathbf{k}; \mathbf{p})\}\,\psi(\mathbf{k}; \mathbf{p}) = \int G(\mathbf{k}; \mathbf{p} \mid \mathbf{k}'; \mathbf{p}')\,\psi(\mathbf{k}'; \mathbf{p}')\,d^3(kp), \tag{93}$$

*Important conclusions about the (π, π) interaction can be obtained from the study of the angular distributions of particles produced in (π, N) collisions. In particular, an indication of the (π, π) interaction will be found in the departure from isotropy in the center-of-mass system for stars in which the multiplicity of the particles produced is small.

where the operator G is defined by

$$G = w\frac{r}{1-r}. \qquad (93')$$

For real processes $E = H_0$, and because of the imaginary character of the function $\delta^+(E-H_0) = (E-H_0)^{-1} - i\pi\delta(E-H_0)$ the matrix r will contribute to the imaginary part of the operator G. Thus the operator G is complex, and this complex character is due to real, inelastic, processes.

Let us now go over to a coordinate system in which $\mathbf{k}+\mathbf{p}=0$. Equation (93) is then written in the form

$$\{E - E_N(q) - E_\pi(q)\}\,\psi(q) = \int G(q|q')\,\psi(q')\,d^3q', \qquad (94)$$

or in the coordinate representation

$$\{E - H_N(x) - H_\pi(x)\}\,\psi(x) = \int F(x|x')\,\psi(x')\,d^3x'. \qquad (95)$$

Here $H_N(x)$ and $H_\pi(x)$ are the Hamiltonians for the free motion of the nucleon and π meson. As we see, the interaction with which we are concerned is determined, in general, by the nonlocal operator $F(x|x')$. If, however, the original system of equations (88) is local, then the nonlocal character in Eq. (95) is only the result of writing in the coordinate representation the fact that the interaction depends on the velocities,

$$\int F(x|x')\,\psi(x')\,d^3x' = V(x;\ E;\ \nabla^2)\,\psi(x), \qquad (96)$$

where V is the complex operator for the interaction, which depends on the velocities of the particles:

$$V(x;\ E;\ \nabla^2) = \sum_k \frac{1}{k!}\int F(\mathbf{x}|\mathbf{x}';E)\left[(\mathbf{x}'-\mathbf{x})\frac{\partial}{\partial \mathbf{n}(x)}\right]^k d^3x'$$

$$= \sum_k \frac{1}{k!}\,V_k(\mathbf{x};\ E)\,\frac{\partial^k}{\partial \mathbf{n}(x)^k},$$

or

$$V(x;\ E;\ \nabla^2) = \sum_k \frac{1}{k!}\,V_k(\mathbf{x};\ E)\cdot\sqrt{\nabla^{2k}}. \qquad (97)$$

B. The Conditions for the Existence of a Complex Potential

We see that, generally speaking, there does not exist a complex potential, which could be interpreted as the optical index of refraction and absorption coefficient of pion waves inside the nucleon, since instead of a potential we get the nonlocal operator $F(\mathbf{x}|\mathbf{x}')$.

In the case in which geometrical optics can be applied, however, we have

$$\psi(x) = \psi_0(x)\,e^{ikx} \text{ and } \frac{\partial\psi_0}{\partial x} \cong 0. \qquad (98)$$

In this case the operator $V(x;\ E;\ \nabla^2)$ reduces to a complex potential depending on the momentum of the particle,

$$V(x;\ E;\ \nabla^2) \to V(x;\ k), \qquad (99)$$

i.e., the conditions for the applicability of geometrical optics coincide with the conditions under which the nonlocal operator F or V can be replaced by the complex potential (99).

In those regions in the nucleon where the absorption becomes so strong that the amplitude of the pion wave changes appreciably in a distance of a wavelength λ, more general relations must be used to calculate the phase shifts η_l. We recall also that the approximation of the optical model improves as we go to shorter wavelengths.

9. CONCLUSION

As can be seen, the study of the structure of elementary particles, and primarily that of nucleons, is still in the very first stages of its development. The aspect that has been furthest advanced is the study of the electromagnetic structures of the proton and neutron. The data that have been obtained on the distributions of charge and magnetic moment in nucleons agree with the basic theoretical ideas of the pion theory. For the central parts of the nucleon, however, the electromagnetic properties still remain very obscure.

The study of the structure of nucleons by means of nuclear interactions is in a still more primitive state.

As of now the simplest and most feasible approach to the mesonic structure of the nucleon is the analysis of the scattering of pions on the basis of the optical model of the nucleon. In its present form this model has physical meaning for sufficiently energetic pions (or nucleons) and for not too deep layers of the structure of the nucleon.

NOTE ADDED IN PROOF

1. The estimate $\sigma_{\pi\pi} \gtrsim 5$ mb in Sec. 7C is a lower limit of the possible values of $\sigma_{\pi\pi}$, obtained when the nucleons and antinucleons into which the π meson disintegrates are regarded as point ("bare") particles. If we take into account their effective dimensions, then the effective size of the π meson, and accordingly the cross section $\sigma_{\pi\pi}$, may become several times this value. The curve $k(r) = \sigma_{\pi\pi}(r)\rho(r)$ in Fig. 12 can then come into agreement with the curve for $k(r)$ obtained from the optical analysis.

2. As has been shown by recent experiments of É. Tsyganov with the proton synchrotron at the Joint Institute (to be published), the angular distribution of elastic (pp) scattering at small angles ($\theta < 10°$ in the center-of-mass system) cannot be explained in terms of a purely absorbing ("black" or "grey") nucleon.

It is possible that at small angles, even at high energies, potential scattering still plays an appreciable role: $d\sigma_{nd}/d\Omega \neq 0$.

[1] H. Yukawa, Proc. Phys. Math. Soc. Japan **17**, 48 (1935).

[2] G. F. Chew, Phys. Rev. **95**, 1669 (1954); G. C. Wick, Revs. Modern Phys. **27**, 339 (1955); H. Miyazawa, Phys. Rev. **101**, 1564 (1956).

[3] R. Jastrow, Phys. Rev. **81**, 165 (1951).

[4] D. I. Blokhintsev, J. Exptl. Theoret. Phys. (U.S.S.R.) **29**, 33 (1955), Soviet Phys. JETP **2**, 23 (1956).

[5] D. I. Blokhintsev, CERN Symposium 1956, vol. 2, 1955.

[6] K. I. Alekseeva and I. L. Grigorov, Dokl. Akad Nauk SSSR **117**, 593 (1957), Soviet Phys.–Doklady **2**, 514 (1958).

[7] R. B. Begzhanov, J. Exptl. Theoret. Phys. (U.S.S.R.) **34**, 775 (1958), Soviet Phys. JETP **7**, 534 (1958).

[8] D. I. Blokhintsev, J. Exptl. Theoret. Phys. (U.S.S.R.) **30**, 672 (1955) [sic!].

[9] V. S. Barashenkov and V. M. Maltsev, Acta Phys. Polonica **17**, 177 (1958).

[10] Blokhintsev, Barashenkov, and Grishin, Nuovo cimento **9**, 249 (1958).

[11] Blokhintsev, Barashenkov, and Grishin, J. Exptl. Theoret. Phys. (U.S.S.R.) **35**, 311 (1958), Soviet Phys. JETP **8**, 215 (1959).

[12] V. G. Grishin, J. Exptl. Theoret. Phys. (U.S.S.R.) **35**, 501 (1958), Soviet Phys. JETP **8**, 345 (1959).

[13] V. S. Barashenkov and Huang Nien-Ning, J. Exptl. Theoret. Phys. (U.S.S.R.) **36**, 832 (1959), Soviet Phys. JETP **9**, 587 (1959).

[14] V. S. Barashenkov, "Optical Analysis of the Interaction of Fast Nucleons and Pions with Nucleons and Nuclei." Conference on Field Theory and Elementary Particles, Uzhgorod, 1958 (in press).

[15] V. S. Barashenkov and Huang Nien-Ning, J. Exptl. Theoret. Phys. (U.S.S.R.) **36**, 1319 (1959), Soviet Phys. JETP **9**, 935 (1959).

[16] E. Werner, Z. Naturforsch. **13**, 238 (1958).

[17] K. K. Saak'yan, Candidate's Dissertation, 1940.

[18] G. Salzman, Phys. Rev. **99**, 973 (1955); **105**, 1076 (1957).

[19] F. Zachariasen, Phys. Rev. **102**, 295 (1956).

[20] Yennie, Lévy, and Ravenhall, Revs. Modern Phys. **29**, 144 (1957).

[21] R. Hofstadter, Revs. Modern Phys. **28**, 214 (1956).

[22] Hofstadter, Bumiller, and Yearian, Revs. Modern Phys. **30**, 482 (1958).

[23] R. Hofstadter, Ann. Rev. Nuc. Sci. **7**, 231 (1957).

[24] M. N. Rosenbluth, Phys. Rev. **79**, 615 (1950).

[25] W. K. H. Panofsky, Report at the Annual International Conference on High Energy Physics at CERN, Geneva 1958.

[26] V. Z. Jankus, Phys. Rev. **102**, 1586 (1956).

[27] Havens, Rabi, and Rainwater, Phys. Rev. **72**, 634 (1947); **82**, 345 (1950).

[28] S. D. Drell, Ann. of Phys. **4**, 75 (1958).

[29] I. M. Zlatev and P. S. Isaev, J. Exptl. Theoret. Phys. (U.S.S.R.) **35**, 309 (1958), Soviet Phys. JETP **8**, 213 (1959).

[30] A. M. Baldin, Report in Venice, 1957.

[31] Barashenkov, Stakhanov, and Aleksandrov, J. Exptl. Theoret. Phys. (U.S.S.R.) **32**, 154 (1957), Soviet Phys. JETP **5**, 144 (1957).

[32] Yu. A. Aleksandrov, J. Exptl. Theoret. Phys. (U.S.S.R.) **32**, 561 (1957) [sic!].

[33] Yu. A. Aleksandrov and V. S. Barashenkov, Reports at the All-Union Conference on Low and Medium Energies, Moscow, 1957.

[34] V. S. Barashenkov and B. M. Barbashov, Nucl. Phys. **9**, 426 (1958).

[35] V. S. Barashenkov and B. M. Barbashov, "Some Remarks on the Internal Structure of the Nucleon," Conference on Field Theory and Elementary Particles, Uzhgorod, 1958 (in press).

[36] S. D. Drell and Fubini, "Higher Electromagnetic Corrections to Electron-Proton Scattering" (preprint).

[37] G. Sandri, Phys. Rev. **101**, 1616 (1956).

[38] I. E. Tamm, J. Exptl. Theoret. Phys. (U.S.S.R.) **32**, 178 (1957), Soviet Phys. JETP **5**, 154 (1957).

[39] V. S. Barashenkov, Nucl. Phys. **7**, 146 (1958); J. Exptl. Theoret. Phys. (U.S.S.R.) **34**, 1016 (1958), Soviet Phys. JETP **7**, 701 (1958).

[40] J. Bernstein and M. L. Goldberger, Revs. Modern Phys. **30**, 465 (1958).

[41] K. Tanaka, Phys. Rev. **109**, 578 (1958); **110**, 1185 (1958).

[42] Chew, Karplus, Gasiorowicz, and Zachariasen, Phys. Rev. **110**, 265 (1958).

[43] S. D. Drell, Report at the Annual International Conference on High Energy Physics at CERN, Geneva 1958.

[44] Bogachev, Bunyatov, Gramenitskiĭ, Lyubimov, Merekov, Podgoretskiĭ, Sidorov, and Tuvdendorzh, Data from a study of the inelastic interaction of

9 Bev protons with nucleons, included in report by V. I. Veksler at the Second Geneva Conference on the Use of Atomic Energy for Peaceful Purposes, September, 1958.

[45] Barashenkov, Belyakov, Wang, Glagolev, Dalkhazhav, Kirillova, Markov, Mal'tsev, Lebedev, Tolstov, Tsyganov, Shafranova, and Yao, "Interaction of 9 Bev Protons with Nuclei in a Photographic Emulsion," J. Atomic Energy (U.S.S.R.) (to be published).

[46] V. S. Barashenkov, "Multiple Production of Particles in Experiments with 9 Bev Protons at the Synchrotron of the Joint Institute of Nuclear Studies," Conference on Field Theory and Elementary Particles, Uzhgorod, 1958 (in press).

[47] V. S. Barashenkov and Huang Nien-Ning, J. Exptl. Theoret. Phys. (U.S.S.R.) **36**, 1319 (1959), Soviet Phys. JETP **9**, 935 (1959).

[48] I. M. Gel'fand and B. M. Levitan, Izv. AN SSSR, Ser. Mat. **15**, 309 (1951).

[49] Marchenko, Izv. AN SSSR **16**, 309 (1951) [sic!].

[50] Krein, Nuovo cimento **8**, 612 (1958) [sic!].

[51] M. Verde, Nuovo cimento **6**, 340 (1957); **8**, 560 (1958).

[52] Grishin, Saitov, and Chuvilo, J. Exptl. Theoret. Phys. (U.S.S.R.) **34**, 1221 (1958), Soviet Phys. JETP **7**, 844 (1958); S. Z. Belen'kii, J. Exptl. Theoret. Phys. (U.S.S.R.) **33**, 1248 (1957), Soviet Phys. JETP **6**, 960 (1958); Ito, Minami, and Tanaka, Nuovo cimento **9**, 208 (1958).

[53] M. A. Markov, Гипероны и *K*-мезоны (Hyperons and K Mesons), Fizmatgiz, 1958.

[54] A. M. Baldin, Nuovo cimento **8**, 569 (1958).

[55] D. I. Blokhintsev, Dokl. Akad. Nauk SSSR **53**, 201 (1946).

[56] A. E. Brenner and R. W. Williams, Phys. Rev. **106**, 1020 (1957).

[57] W. Pauli, Meson Theory of Nuclear Forces, Interscience, N. Y. 1946 (Russ. Transl. IL, 1957).

[58] B. S. Neganov, J. Exptl. Theoret. Phys. (U.S.S.R.) **33**, 260 (1957); **105**, 1934 (1957) [sic!].

[59] A. Petermann, Helv. Phys. Acta **27**, 441 (1954); R. P. Feynman and G. Speisman, Phys. Rev. **94**, 500 (1954).

[60] Barashenkov, Mal'tsev, and Makhul (in press).

Translated by W. H. Furry